

See discussions, stats, and author profiles for this publication at: <https://www.researchgate.net/publication/47677553>

Exploring the Emissive Properties of New Azacrown Compounds Bearing Aryl, Furyl, or Thienyl Moieties: A Special Case of Chelation Enhancement of Fluorescence upon Interaction with...

ARTICLE *in* INORGANIC CHEMISTRY · NOVEMBER 2010

Impact Factor: 4.76 · DOI: 10.1021/ic101095y · Source: PubMed

CITATIONS

12

READS

17

5 AUTHORS, INCLUDING:



Elisabete Oliveira

University of Vigo

46 PUBLICATIONS 513 CITATIONS

SEE PROFILE



Rosa M F Batista

University of Minho

37 PUBLICATIONS 661 CITATIONS

SEE PROFILE



Maria Manuela M Raposo

University of Minho

125 PUBLICATIONS 2,139 CITATIONS

SEE PROFILE



Carlos Lodeiro

University NOVA of Lisbon

240 PUBLICATIONS 3,058 CITATIONS

SEE PROFILE

Exploring the Emissive Properties of New Azacrown Compounds Bearing Aryl, Furyl, or Thienyl Moieties: A Special Case of Chelation Enhancement of Fluorescence upon Interaction with Ca^{2+} , Cu^{2+} , or Ni^{2+}

Elisabete Oliveira,[†] Rosa M. F. Baptista,[‡] Susana P. G. Costa,[‡] M. Manuela M. Raposo,^{*,‡} and Carlos Lodeiro^{*,†,§}

[†]REQUIMTE, Department of Chemistry, FCT-UNL, 2829-516 Monte de Caparica, Portugal, [‡]CQ-UM, Center of Chemistry, University of Minho, Campus Gualtar, 4710-057 Braga, Portugal, and [§]BIOSCOPE Research Team, Faculty of Science, Physical-Chemistry Department, Campus Ourense, University of Vigo, 32004, Ourense, Spain.

Received May 31, 2010

Three new compounds bearing furyl, aryl, or thienyl moieties linked to an imidazo-crown ether system (**1**, **2**, and **3**) were synthesized and fully characterized by elemental analysis, infrared, UV–vis absorption, and emission spectroscopy, X-ray crystal diffraction, and MALDI-TOF-MS spectrometry. The interaction toward metal ions (Ca^{2+} , Cu^{2+} , Ni^{2+} , and Hg^{2+}) and F^- has been explored in solution by absorption and fluorescence spectroscopy. Mononuclear and binuclear metal complexes using Cu^{2+} or Hg^{2+} as metal centers have been synthesized and characterized. Compounds **2** and **3** show a noticeable enhancement of the fluorescence intensity in the presence of Ca^{2+} and Cu^{2+} ions. Moreover compound **3** presents a dual sensory detection way by modification of the fluorimetric and colorimetric properties in the presence of Cu^{2+} or Hg^{2+} . EPR studies in frozen solution and in microcrystalline state of the dinuclear $\text{Cu}(\text{II})$ **3** complex revealed the presence of an unique Cu^{2+} type.

Introduction

Classically a fluorescent chemosensor is a molecular device formed by an ionophore, a fluorophore, and a chemical spacer in between.¹ On the basis of this basic architectural premise, the field of fluorescence chemosensors has grown during recent years due to their importance in applications, such as in material sciences, biomedical, analytical chemistry, and environmental sciences.²

Pioneering studies by H.G. Löhr and F. Vögtle on the properties of chromo and fluoroinophoric dyes,³ and the studies by Okamoto on the chemiluminescent behaviors of several crown-ether-modified Iophine peroxide ionophore,⁴

increased notably the knowledge on crown-ether derivatives as metal ion chemosensors.

Incorporation of the imidazole group in abiotic systems has been extensively explored since the initial work of Debus in 1858⁵ because of their interesting chemical and biochemical properties. These compounds have important pharmacological properties and play an important role in many biochemical processes, such as inhibitors of P38 MAP kinase, fungicides or herbicides, and therapeutic agents.⁶

Besides their classical applications in medicinal chemistry,⁶ 2,4,5-triaryl(heteroaryl)-imidazoles play also important roles in materials science because of their optoelectronic properties.⁷ Recently, triaryl(heteroaryl)-imidazole-based chromophores have received increasing attention because of their distinctive linear and nonlinear optical properties and also because of their excellent thermal stability in guest–host systems. Therefore, they have found application as nonlinear optical materials,^{7a–j} fluorescent chemosensors,^{7k–m} two-photon absorbing molecules,⁷ⁿ and thermally stable luminescent materials for several applications such as OLEDs.⁷

Earlier studies on triaryl(heteroaryl)-imidazoles showed that the fluorescence properties of these derivatives could

*Authors to whom correspondence should be addressed. E-mail: mfox@quimica.uminho.pt (M.M.M.R.); clodeiro@uvigo.es (C.L.). Fax: +351 253 604382 (M.M.M.R.); +34 988 387001 (C.L.).

(1) (a) Czarnik, A. W. *Acc. Chem. Res.* **1994**, *27*, 302–308. (b) Czarnik, A. W. *Acc. Chem. Res.* **1998**, *31*, 201–207.

(2) (a) Ulijn, R. V.; Smith, A. M. *Chem. Soc. Rev.* **2008**, *37*, 664–675. (b) Cavalli, S.; Albericio, F.; Kros, A. *Chem. Soc. Rev.* **2010**, *39*, 241–263. (c) Sawada, T.; Takahashi, T.; Mihara, H. *J. Am. Chem. Soc.* **2009**, *131*(40), 14434–14441. (d) Lodeiro, C.; Pina, F. *Coord. Chem. Rev.* **2009**, *253*, 1353–1383. (e) Prodi, L.; Bolleta, F.; Montalti, M.; Zaccheroni, N. *Coord. Chem. Rev.* **2000**, *205*, 59–83. (f) Martínez-Mañez, M.; Sancenó, F. *Chem. Rev.* **2003**, *103*, 4419–4476. (g) Jiang, P. J.; Guo, Z. J. *Coord. Chem. Rev.* **2004**, *248*, 205–229. (h) Finney, N. S. *Current Opp. Chem. Biol.* **2006**, *10*, 238–245.

(3) Löhr, H. G.; Vögtle, F. *Acc. Chem. Res.* **1985**, *18*, 65–72.

(4) Okamoto, H.; Owari, M.; Kimura, M.; Satake, K. *Tetrahedron Lett.* **2001**, *42*, 7453–7455.

(5) Debus, H. *Liebigs Ann. Chem.* **1858**, *107*, 199–208.

(6) (a) Siddiqui, S. A.; Narkhede, U. C.; Palimkar, S. S.; Daniel, T.; Rajgopal, J. L.; Srinivasan, K. V. *Tetrahedron* **2005**, *61*, 3539–3546 and references therein. (b) Bellina, F.; Cauteruccio, S.; Rossi, R. *Tetrahedron* **2007**, *63*, 4571–4624 and references therein.

be tuned by substitution of the aryl group at the position 2 by a 5-membered heterocyclic ring such as thiophene or thiazole.^{7n,o,q-r} It is expected that the use of five-membered heteroaromatics such as thiophenes and thiazoles in the conjugation pathway should minimize the distortion of conjugation between the imidazole ring and the aromatic ring at the position 2, thus enhancing conjugation and the charge transport properties along the oligomer backbone.^{7o,q,r} Therefore, a comparative study of the fluorescence properties for several 2,4,5-triaryl(heteroaryl)-imidazoles showed that the substitution of the 2-phenyl ring in 2,4,5-triphenyl-imidazole by a thiophene or a thiazole improved the fluorescence quantum yields, from 0.48 to 0.86 in the case of thiophene or to 0.57 in the case of the thiazole, due to a more planar conformation of the heterocyclic imidazoles.^{7r}

In addition the study of the effect of *N*-alkylation of the imidazole ring on the fluorescent properties of 2,4,5-triaryl(hetero)aryl-imidazoles showed a significant fluorescence reduction for the 1-substituted derivatives. However, the fluorescence decrease is noticeably much smaller for imidazoles having thiophene or thiazoles in position 2 because of the higher planarity of these conjugated systems.^{7r}

Among other analytical techniques, fluorescence spectroscopy has been extensively applied for the study of the interaction of natural or artificial chemosensors with metal ions, mainly due to higher sensibility and sensitivity achieved and for being a nondestructive technique.^{8,9}

The general interest on the detection of bioinorganic metal ions, such as Ca^{2+} , Cu^{2+} , and even Ni^{2+} is the result of the difference in the electronic properties of these metals, which leads to different recognition mechanisms that can be followed by fluorimetry.¹⁰ For example, Ca^{2+} , as an alkaline-

earth metal ion, is normally recognized by the enhancement in the fluorescence intensity (CHEF effect),¹¹ while paramagnetic transition metal ions or heavy metals, such as Cu^{2+} , Ni^{2+} , and Hg^{2+} , with unfilled d shells orbitals are usually recognized by a chelation enhancement of the quenching (CHEQ effect), via an electron- or an energy-transfer mechanism. Among these, Hg^{2+} as a diamagnetic d¹⁰ metal is an exception, for which the quenching could also be caused by the spin-orbit coupling, being the main route for the non-radiative deactivation k_{nr} process.¹²

However, few examples are reported in the literature for the recognition of Cu^{2+} , Ni^{2+} , or Hg^{2+} by fluorescence enhancement,¹³ and so, the development of new sensors for Cu^{2+} , Ni^{2+} , and Hg^{2+} by CHEF recognition is a key topic in chemosensor research.

Following our current interests on colorimetric and fluorimetric chemosensors for metal ion detection provided with heterocyclic moieties bearing N, O, and S donor atoms,¹⁴ and having in mind earlier studies concerning the optical properties of 2,4,5-tri(hetero)aryl-imidazole derivatives, we decided to synthesize and characterize three new imidazo-crown ether derivatives bearing a furyl (**1**), aryl (**2**), or thienyl (**3**) ring

(7) (a) Moylan, C. R.; Miller, R. D.; Twieg, R. J.; Betterton, K. M.; Lee, V. Y.; Matray, T. J.; Nguyen, C. *Chem. Mat.* **1993**, *5*, 1499. (b) Bu, X. R.; Li, H. Y.; VanDerveer, D.; Mintz, E. A. *Tetrahedron Lett.* **1996**, *37*, 7331. (c) Santos, J.; Mintz, E. A.; Zehnder, O.; Bosshard, C.; Bu, X. R.; Gunter, P. *Tetrahedron Lett.* **2001**, *42*, 805. (d) Wang, S.; Zhao, L.; Xu, Z.; Wu, C.; Cheng, S. *Mater. Letters* **2002**, *56*, 1035. (e) Wu, W.; Ye, C.; Wang, D. *Arkivoc* **2003**, *59*. (f) Wu, W.; Zhang, Z.; Zhang, X. *J. Chem. Res.* **2004**, *9*, 617. (g) Wu, W.; Zhang, Z. L.; Zhang, X. Y. *J. Nonlinear Opt. Phys. Mater.* **2005**, *14*, 61. (h) Ren, J.; Wang, S. M.; Wu, L. F.; Xu, Z. X.; Dong, B. H. *Dyes Pigments* **2008**, *76*, 310. (i) Batista, R. M. F.; Costa, S. P. G.; Belsley, M.; Lodeiro, C.; Raposo, M. M. M. *Tetrahedron* **2008**, *64*, 9230. (j) Batista, R. M. F.; Costa, S. P. G.; Belsley, M.; Raposo, M. M. M. *Dyes Pigments* **2009**, *80*, 329. (k) Feng, K.; Hsu, F. L.; Bota, K.; Bu, X. R. *Microchem. J.* **2005**, *81*, 23. (l) Zhang, M.; Li, M.; Zhao, Q.; Li, F.; Zhang, D.; Zhang, J.; Yi, T.; Huang, C. *Tetrahedron Lett.* **2007**, *48*, 2329. (m) Zhang, M.; Li, M. Y.; Li, F. Y.; Cheng, Y. F.; Zhang, J. P.; Yi, T.; Huang, C. H. *Dyes Pigments* **2008**, *77*, 408. (n) Feng, K.; De Boni, L.; Misoguti, L.; Mendonça, C. R.; Meador, M.; Hsu, F. L.; Bu, X. R. *Chem. Commun.* **2004**, 1178. (o) Zhao, L.; Li, S. B.; Wen, G. A.; Peng, B.; Huang, W. *Mater. Chem. Phys.* **2006**, *100*, 460. (p) Fang, Z.; Wang, S.; Zhao, L.; Xu, Z.; Ren, J.; Wang, X.; Yang, Q. *Mater. Chem. Phys.* **2008**, *107*, 305. (q) Pina, J.; Seixas de Melo, J.; Batista, R. M. F.; Costa, S. P. G.; Raposo, M. M. M. *J. Phys. Chem. B* **2010**, *114*, 4964. (r) Feng, K.; Hsu, F. L.; Van DerVeer, D.; Bota, K.; Bu, X. R. *J. Photochem. Photobiol. A-Chem.* **2004**, *165*, 223.

(8) De Silva, A. P.; Gunaratne, H. Q. N.; Gunnlaugsson, T.; Huxley, A. J. M.; McCoy, C. P.; Rademacher, J. T.; Rice, T. E. *Chem. Rev.* **1997**, *97*, 1515–1566.

(9) (a) Bolletta, F.; Costa, I.; Fabbri, L.; Licchelli, M.; Montalti, M.; Pallavicini, P.; Prodi, L.; Zaccaroni, N. *J. Chem. Soc., Dalton Trans.* **1999**, 1381–1386. (b) Goldsmith, C. R.; Lippard, S. J. *Inorg. Chem.* **2006**, *45*, 6474–6478. (c) Wu, D.; Huang, W.; Duan, C.; Zhihua, L.; Meng, Q. *Inorg. Chem.* **2007**, *46*, 1538–1540. (d) Alarcon, J.; Albelda, M. T.; Belda, R.; Clares, M. R.; Delgado-Pinar, E.; Frias, J. C.; García-España, E.; González, J.; Soriano, C. *Dalton Trans.* **2008**, *46*, 6530–6538. (e) Mameli, M.; Aragoni, M. C.; Arca, M.; Caltagirone, C.; Demartin, F.; Farrugia, G.; De Filippo, G.; Devillanova, F. A.; Garau, A.; Isaia, F.; Lippolis, V.; Murgia, S.; Prodi, L.; Pintus, A.; Zaccaroni, N. *Chem.—Eur. J.* **2010**, *16*, 919–930.

(10) Rurack, K. *Spectrochim. Acta A* **2001**, *57*, 2161–2195.

(11) (a) Kim, J.; Morozumi, T.; Nakamura, H. *Org. Lett.* **2007**, *9*, 4419–4422. (b) Magri, D. C.; Callan, J. F.; de Silva, A. P.; Fox, D. B.; McClenaghan, N. D.; Sandanayake, K. R. A. S. *J. Fluoresc.* **2005**, *15*, 769–775. (c) Vysotski, E. S.; Lee, J. *Acc. Chem. Res.* **2004**, *37*, 405–415. (d) Parkers, R.; Mohsin, S.; Lee, T. C.; Gunnlaugsson, T. *Chem. Mater.* **2007**, *19*, 1656–1663. (e) Gerencser, A. A.; Adam-Vizi, V. *Cell Calcium* **2001**, *30*, 311–321.

(12) (a) Boiocchi, M.; Fabbri, L.; Licchelli, M.; Sacchi, D.; Vázquez, M.; Zampa, C. *Chem. Commun.* **2003**, 1812–1813. (b) Anda, C.; Bazzicalupi, C.; Bencini, A.; Bianchi, A.; Fornasari, P.; Giorgi, C.; Valtancoli, B.; Lodeiro, C.; Parola, A. J.; Pina, F. *Dalton Trans.* **2003**, 1299–1307. (c) Nuñez, C.; Bastida, R.; Macias, A.; Bértolo, E.; Fernandes, L.; Capelo, J. L.; Lodeiro, C. *Tetrahedron* **2009**, *65*, 6179–6188. (d) Tamayo, A.; Lodeiro, C.; Escriche, L.; Casabo, J.; Covelo, B.; González, P. *Inorg. Chem.* **2005**, *44*, 8105–8115. (e) Fernandes, L.; Boucher, M.; Fernández-Lodeiro, J.; Oliveira, E.; Nuñez, C.; Santos, H. M.; Capelo, J. L.; Faza, O. N.; Bértolo, E.; Lodeiro, C. *Inorg. Chem. Commun.* **2009**, *12*, 905–912. (f) Aragoni, M. C.; Arca, M.; Bencini, A.; Blake, A. J.; Caltagirone, C.; Decortes, A.; Demartin, F.; Devillanova, F. A.; Faggi, E.; Dolci, L. S.; Garau, A.; Isaia, F.; Lippolis, V.; Prodi, L.; Valtancoli, B.; Zaccaroni, N. *Dalton Trans.* **2005**, 2994–3004.

(13) (a) Yu, M.; Shi, M.; Chen, Z.; Li, F.; Li, X.; Gao, Y.; Xu, J.; Yang, H.; Zhou, Z.; Yi, T.; Huang, C. *Chem.—Eur. J.* **2008**, *14*, 6892–6900. (b) Xu, Z.; Xiao, Y.; Qian, X.; Cui, J.; Cui, D. *Org. Lett.* **2005**, *7*, 889–892. (c) Chem, X. Q.; Jia, J.; Ma, H. M.; Wang, S. J.; Wang, X. C. *Anal. Chim. Acta* **2009**, *1*, 9–14. (d) Wang, H. X.; Wang, D. L.; Wang, Q.; Li, X. Y.; Schalley, C. A. *Org. Biomol. Chem.* **2010**, *8*, 1017–1026. (e) Yang, Y. K.; Yook, K. J.; Tae, J. *J. Am. Chem. Soc.* **2005**, *127*, 16760–16761. (f) Zhang, G.; Zhang, D.; Yin, S.; Yang, X.; Shuai, Z.; Zhu, D. *Chem. Commun.* **2005**, *16*, 2161–2163. (g) Guo, X.; Qian, X.; Jia, L. *J. Am. Chem. Soc.* **2004**, *126*, 2272–2273. (h) Nolan, E. M.; Lippard, S. J. *J. Am. Chem. Soc.* **2003**, *125*, 14270–14721. (i) Henrich, G.; Walther, W.; Resch-Genger, U.; Sonnenschein, H. *Inorg. Chem.* **2001**, *40*, 641–644. (j) Zhao, Y.; Lin, Z.; He, C.; Wu, H.; Duan, C. *Inorg. Chem.* **2006**, *45*, 10013–10015. (k) Shamsipur, M.; Hosseini, M.; Alixadeh, K.; Alizadeh, N.; Yari, A.; Caltagirone, C.; Lippolis, V. *Anal. Chim. Acta* **2005**, *353*, 17–24. (l) Goretzki, G.; Bonnesen, P. V.; Dabestain, R.; Brown, G. M. *ACS Symp. Ser.* **2008**, *943*, 13–33. (m) Al-Kady, A. S.; Gaber, M.; Hussein, M. M.; Ebeid, E. Z. M. *J. Phys. Chem. A* **2009**, *34*, 9474–9478. (n) Lee, Y. J.; Seo, D.; Kwom, J. Y.; Son, G.; Park, M. S.; Choi, Y.-H.; Soh, J. H.; Lee, H. N.; Lee, K. D.; Yoon, J. *Tetrahedron* **2006**, *62*, 12340–12344. (o) Chandrasekhar, V.; Bag, P.; Pandey, M. D. *Tetrahedron* **2009**, *65*, 9876–9883.

(14) (a) Batista, R. M. F.; Oliveira, E.; Nuñez, C.; Costa, S. P. G.; Lodeiro, C.; Raposo, M. M. M. *J. Phys. Org. Chem.* **2009**, *22*, 362–366. (b) Pedras, B.; Fernandes, L.; Oliveira, E.; Rodríguez, L.; Raposo, M. M. M.; Capelo, J. L.; Lodeiro, C. *Inorg. Chem. Commun.* **2009**, *12*, 79–85. (c) Batista, R. M. F.; Oliveira, E.; Costa, S. P. G.; Lodeiro, C.; Raposo, M. M. M. *Org. Lett.* **2007**, *9*, 3201–3204. (d) Costa, S. P. G.; Oliveira, E.; Lodeiro, C.; Raposo, M. M. M. *Sensors* **2007**, *7*, 2096–2114. (e) Lodeiro, C.; Capelo, J. L.; Mejuto, J. C.; Oliveira, E.; Santos, H. M.; Pedras, B.; Nuñez, C. *Chem. Soc. Rev.* **2010**, *39*, 2948–2976. (f) Raposo, M. M. M.; García-Acosta, B.; Ábalos, T.; Martínez-Manez, R.; Ros-Lis, J. V.; Soto, J. J. *Org. Chem.* **2010**, *75*, 2922–2933.

linked via the imidazo unit to the azacrown ether system, in order to tune their photophysical properties and evaluate their chemosensor ability.

The interaction with Ca^{2+} , Cu^{2+} , Ni^{2+} , and Hg^{2+} in solution and in solid state was explored using absorption and fluorescence spectroscopy, electron paramagnetic resonance (EPR), and MALDI-TOF-MS spectrometry. To explore the acid–base behavior of these systems, interaction with H^+ and a basic anion, F^- , were also studied. The X-ray crystallographic structure of compound **2** is also reported.

Experimental Section

Materials and Apparatus. Reaction progress was monitored by thin layer chromatography (0.25 mm thick precoated silica plates: Merck Fertigplatten Kieselgel 60 F254), while purification was performed by silica gel column chromatography (Merck Kieselgel 60; 230–400 mesh). NMR spectra of the ligands were obtained on a Varian Unity Plus Spectrometer at an operating frequency of 300 MHz for ^1H NMR and 75.4 MHz for ^{13}C NMR or a Bruker Avance III 400 at an operating frequency of 400 MHz for ^1H NMR and 100.6 MHz for ^{13}C NMR using the solvent peak as internal reference. The solvents are indicated in parentheses before the chemical shift values (δ relative to tetramethylsilane and given in ppm). Melting points were determined on a Gallenkamp apparatus and are uncorrected. Infrared spectra were recorded on a BOMEM MB 104 or a JASCO IR spectrophotometer. Mass spectrometry analyses of the ligands were performed at the “C.A.C.T.I.—Unidad de Espectrometría de Masas” at the University of Vigo, Spain. Elemental analyses were carried out by the REQUIMTE DQ, Universidade Nova de Lisboa Service on a Thermo Finnigan-CE Flash-EA 1112-CHNS Instrument. Proton ^1H NMR of the complexes were recorded on a Bruker Avance III 400 at an operating frequency of 400 MHz. The MALDI analysis has been performed in a MALDI-TOF-MS model Voyager-DE 4700 Proteomics Analyzer, by positive reflector mode, at the REQUIMTE, Chemistry Department, Universidade Nova de Lisboa.

Spectrophotometric and Spectrofluorimetric Measurements. Absorption spectra were recorded on a Perkin-Elmer lambda 45 spectrophotometer and fluorescence on a Perkin-Elmer L55. The linearity of the fluorescence vs concentration was checked in the concentration used (10^{-4} – 10^{-6} M). A correction for the absorbed light was performed when necessary. Stock solutions of the compounds ($\sim 10^{-3}$ M) were prepared in absolute ethanol and acetonitrile for **1**, and in absolute ethanol, acetonitrile, and dichloromethane for **2** and **3**. Titrations of ligands **1**, **2**, and **3** (10^{-5} – 10^{-6} M, prepared by dilution of the stock solutions) were carried out by the addition of microliter amounts of standard solutions of the ions in absolute ethanol or acetonitrile. All the measurements were performed at 298 K. The competition experiments were carried out on a JASCO 650 UV–vis spectrometer and on a Horiba-Jovin Ibon Fluoromax 4 spectrofluorimeter.

Luminescence quantum yields were measured using a solution of quinine sulfate in sulphuric acid (0.5M) as a standard¹⁵ [ϕ] = 0.54 and were corrected for different refraction indexes of solvents,^{15b} for compounds **2** and **3**. For compound **1**, the relative quantum yield was measurement using an ethanol solution of anthracene as standard [ϕ] = 0.27.¹⁵

EPR Measurements. EPR measurements were performed in the REQUIMTE, Universidade NOVA de Lisboa at 70 K in both finely powdered and ethanol dissolved samples at 9.65

Table 1. Crystal Data and Structure Refinement for Ligand **2**

empirical formula	$\text{C}_{31}\text{H}_{35}\text{N}_3\text{O}_4$
formula weight	513.62
temperature	293(2) K
wavelength	0.71073 Å
crystal system	tetragonal
space group	$P4/ncc$
unit cell dimensions	$a = 28.201(11)$ Å, $\alpha = 90^\circ$ $b = 28.201(11)$ Å, $\beta = 90^\circ$ $c = 15.453(12)$ Å, $\gamma = 90^\circ$
volume	$12290.5(12)$ Å ³
Z	16
density (calculated)	1.110 g/cm ³
absorption coefficient	0.074 mm ⁻¹
$F(000)$	4384
crystal size	$0.50 \times 0.46 \times 0.30$ mm ³
θ range for data collection	2.04 – 24.99°
index ranges	$-33 \leq h \leq 32$, $-25 \leq k \leq 33$, $-18 \leq l \leq 18$
reflections collected	40683
independent reflections	5300 [$R_{\text{int}} = 0.0684$]
completeness to θ	97.7% (24.99°)
absorption correction	empirical (SADABS)
refinement method	full-matrix least-squares on F^2
data/restraints/parameters	5300/0/343
goodness-of-fit on F^2	1.069
final R indices [$I > 2\sigma(I)$]	$R1 = 0.0704$, $wR2 = 0.2291$
R indices (all data)	$R1 = 0.1441$, $wR2 = 0.2516$
largest diff. peak and hole	$0.341/-0.206$ e Å ⁻³

GHz with a Bruker EMX spectrometer using a rectangular cavity equipped with an Oxford continuous helium flow cryostat. Modulation field: 5 Gpp. Modulation frequency: 100 kHz. Attenuation: 30 dB (200 microW).

X-ray Crystal Structure Determination. Single crystals of ligand **2** was analyzed by X-ray diffraction and a summary of the crystallographic data and the structure refinement parameters is reported in Table 1.

Crystallographic data were collected on a Bruker Smart 1000 CCD diffractometer at CACTI (Universidade de Vigo) at 20 °C using graphite monochromated Mo K α radiation ($\lambda = 0.71073$ Å) and were corrected for Lorentz and polarization effects. The software SMART¹⁶ was used for collecting frames of data, indexing reflections, and the determination of lattice parameters, SAINT¹⁷ for integration of intensity of reflections and scaling, and SADABS¹⁸ for empirical absorption correction. The structures were solved by direct methods using the program SHELXS97.¹⁹ All non-hydrogen atoms were refined with anisotropic thermal parameters by full-matrix least-squares calculations on F^2 using the program SHELXL97.²⁰ Hydrogen atoms were inserted at calculated positions and constrained with isotropic thermal parameters. The contribution of the disordered solvent to the diffraction pattern that could not be rigorously included in the crystallographic calculations, were subtracted by the SQUEEZE procedure implemented in the PLATON software.²¹ Drawings were produced with PLATON6 software (ellipsoids and ball and stick).

Crystallographic data have been deposited with the Cambridge Crystallographic Data Centre, CCDC 730341 for **2**. Copies of this information may be obtained free of charge from The

(16) SMART: Instrument Control and Data Collection Software, version 5.054; Bruker Analytical X-ray Systems Inc.: Madison, WI, 1997.

(17) SAINT: Data Integration software package, version 6.01; Bruker Analytical X-ray Systems Inc.: Madison, WI, 1997.

(18) Sheldrick, G. M. SADABS. A Computer Program for Absorption Corrections; University of Göttingen: Göttingen, Germany, 1996.

(19) Sheldrick, G. M. SHELXS97. A Computer Program for the Solution of Crystal Structures from X-ray Data; University of Göttingen: Göttingen, Germany, 1997.

(20) Sheldrick, G. M. SHELXL97. A Computer Program for the Refinement of Crystal Structures from X-ray Data; University of Göttingen: Göttingen, Germany, 1997.

(21) Spek, A. L. PLATON. A Multipurpose Crystallographic Tool; Utrecht University; Utrecht, The Netherlands, 2001.

(15) (a) Berlman, I. B. *Handbook of Fluorescence Spectra of Aromatic Molecules*, 2nd ed.; Academic Press: New York, 1971. (b) Montalti, L.; Credi, A.; Prodi, T.; Gandolfi, M. T.; *Handbook of Photochemistry*, 3rd ed.; Taylor and Francis Group: Boca Raton, FL, 2006.

Director, CCDC, 12 Union Road, Cambridge, CB2 1EZ, UK (fax: +44-1223-336033; e-mail: deposit@ccdc.cam.ac.uk or http://www.ccdc.ac.uk).

Chemicals and Starting Materials. $\text{Na}(\text{BF}_4)$, $\text{Ca}(\text{CF}_3\text{COO})_2$, $\text{Cu}(\text{BF}_4)_2$, $\text{Ni}(\text{BF}_4)_2$, $\text{Hg}(\text{CF}_3\text{COO})_2$ metal salts, $\text{F}(\text{NBu}_4)$, and $\text{CH}_3\text{SO}_3\text{H}$ have been purchased from Stream Chemicals, Sigma Aldrich, or Solchemar. All solvents used were spectroscopic grade from Chromasolv or PANREAC without any further purification.

Synthesis of Ligands. **Synthesis of 4-(1,4,10,13-Tetraoxa-7-azacyclopentadecan-7-yl)benzaldehyde IV.** POCl_3 (1.20 mmol) was added to DMF (1.20 mmol) at 0 °C, and the mixture was stirred for 15 min at 0 °C. 13-Phenyl-1,4,7,10-tetraoxa-13-azacyclopentadecane (1.03 mmol) dissolved in DMF (1 mL) was added dropwise with stirring. The reaction mixture was heated for 2 h at 60 °C. The solution was then poured slowly into 5 mL saturated sodium acetate aqueous solution and stirred during 30 min. The organic layer was diluted with ether, washed with saturated NaHCO_3 aqueous solution, and dried with anhydrous MgSO_4 . The organic extract was filtered and evaporated under reduced pressure giving the 4-(1,4,10,13-tetraoxa-7-azacyclopentadecan-7-yl)benzaldehyde **IV**²² as a yellow solid in 90% yield.

^1H NMR (300 MHz, CDCl_3): δ 3.61 (m, 16H, $8 \times \text{CH}_2$), 3.70 (m, 4H, $2 \times \text{CH}_2$), 6.66 (d, 2H, $J = 9$ Hz, 2 and 6-H), 7.66 (d, 2H, $J = 9$ Hz, 3 and 5-H), 9.67 (s, 1H, CHO).

General Procedure for the Synthesis of 2,4,5-Tri(hetero)aryl-imidazo Crown Ether Ligands (1–3). A mixture of the formyl azacrown ether **IV** (0.35 mmol), NH_4OAc (10 equiv) and 1,2-diones **I–III** (0.35 mmol) in glacial acetic acid (20 mL) (Method A) or in ethanol (20 mL) (Method B) was stirred and heated at reflux for 12 h. The mixture was then cooled to room temperature and the product precipitated during neutralization with NH_4OH 5 M. The crude product was purified through column chromatography on silica using chloroform/methanol (9:1) as eluent.

7-(4-(4,5-Di(furan-2-yl)-1H-imidazol-2-yl)phenyl)-1,4,10,13-tetraoxa-7-azacyclopentadecane 1. Compound **1** was obtained as a brown solid (Method B, 58%). MP: (94.2–95.8) °C. UV-vis (EtOH): $\lambda_{\text{exc}} = 328$ nm, $\log \epsilon_{328 \text{ nm}} = 4.69$. Emission (EtOH): $\lambda_{\text{em}} = 400$ nm, $\phi = 0.87$. IR (cm^{-1} ; liquid film): ν 3125, 3006, 2870, 1614, 1495, 1392, 1355, 1295, 1205, 1123, 1008, 885, 820, 753. ^1H NMR (300 MHz, acetone- d_6): δ 3.57 (m, 16H, $8 \times \text{CH}_2$), 3.73 (m, 4H, $2 \times \text{CH}_2$), 6.55 (m, 2H, $2 \times 4'$ -H), 6.74 (d, 2H, $J = 7.2$ Hz, 2 and 6-H), 6.73 (dd, 2H, $J = 4$ and 0.8 Hz, $2 \times 3'$ -H), 7.60 (dd, 2H, $J = 2$ and 0.8 Hz, $2 \times 5'$ -H), 7.98 (d, 2H, $J = 7.2$, 3 and 5-H). ^{13}C NMR (75.4 MHz, acetone- d_6): δ 53.11 (CH_2), 69.17 (CH_2), 70.55 (CH_2), 70.79 (CH_2), 71.76 (CH_2), 107.86 ($2 \times \text{C}_{3'}$), 112.06 (C_2 and C_6), 112.22 ($2 \times \text{C}_{4'}$), 118.06 (C_4), 127.87 (C_3 and C_5), 148.35 (C_2), 148.70 (C_{3a} and C_{3b}), 149.23 (C_2). MS (FAB) m/z (%): 494 ($[\text{M} + \text{H}]^+$, 100), 234 (8). HRMS m/z (FAB) for $\text{C}_{27}\text{H}_{31}\text{N}_3\text{O}_6$ calcd 494.22785; found 494.22856.

7-(4-(4,5-Diphenyl-1H-imidazol-2-yl)phenyl)-1,4,10,13-tetraoxa-7-azacyclopentadecane 2. Compound **2** was obtained as a yellow solid (45% method A; 64% method B). MP (178.4–179.2) °C. UV-vis (EtOH): $\lambda_{\text{exc}} = 320$ nm, $\log \epsilon_{320 \text{ nm}} = 4.64$. Emission (EtOH): $\lambda_{\text{em}} = 420$ nm, $\phi = 0.35$. IR (cm^{-1} ; liquid film): ν 3224, 3008, 2870, 1734, 1614, 1508, 1495, 1390, 1355, 1216, 1123, 821, 756, 697. IR (cm^{-1} ; KBr pellet): ν 3189, 1614, 1510–1495, 1122. ^1H NMR (300 MHz, acetone- d_6): δ 3.59 (m, 16H, $8 \times \text{CH}_2$), 3.75 (m, 4H, $2 \times \text{CH}_2$), 6.77 (d, 2H, $J = 9$ Hz, 2 and 6-H), 7.26 (m, 2H, $2 \times 4'$ -H), 7.33 (m, 4H, $2 \times (3'$ and $5'$ -H), 7.58 (m, 4H, $2 \times (2'$ and $6'$ -H), 7.94 (d, 2H, $J = 9$ Hz, 3 and 5-H). ^{13}C NMR (75.4 MHz, acetone- d_6): δ 53.16 (CH_2), 69.27 (CH_2), 70.62 (CH_2), 70.84 (CH_2), 71.84 (CH_2), 112.13 (C_2 and C_6), 119.14 (C_4), 127.41 ($2 \times (\text{C}_3$ and

$\text{C}_5)$, 127.56 ($2 \times \text{C}_{4'}$), 128.62 ($2 \times \text{C}_{2'}$ and $\text{C}_{6'}$), 129.04 ($2 \times (\text{C}_{3'}$ and $\text{C}_{5'})$), 147.79 (C_2), 148.91 (C_1). MS (FAB) m/z (%): 514 ($[\text{M} + \text{H}]^+$, 100), 222 (8). HRMS m/z (FAB) for $\text{C}_{31}\text{H}_{35}\text{N}_3\text{O}_4$ calcd 514.26955; found 514.27003.

7-(4-(4,5-Di(thien-2-yl)-1H-imidazol-2-yl)phenyl)-1,4,10,13-tetraoxa-7-azacyclopentadecane (3). The compound was isolated as a yellow solid (20% method A, 47% method B). MP (213.1–214.6) °C. UV-vis (EtOH): $\lambda_{\text{exc}} = 325$ nm, $\log \epsilon_{320 \text{ nm}} = 4.55$. Emission (EtOH): $\lambda_{\text{em}} = 440$ nm, $\phi = 0.09$. IR (cm^{-1} ; liquid film): ν 3101, 1615, 1508, 1392, 1353, 1297, 1251, 1212, 1121, 988, 934, 819, 689. IR (cm^{-1} ; KBr pellet): ν 3110, 1616, 1511–1495, 1122. ^1H NMR (300 MHz, CDCl_3): δ 3.56 (m, 16H, $8 \times \text{CH}_2$), 3.76 (m, 4H, $2 \times \text{CH}_2$), 6.78 (d, 2H, $J = 9.0$ Hz, 2 and 6-H), 7.07 (m, 2H, $2 \times 4'$ -H), 7.30 (dd, 2H, $J = 4$ and 1.2 Hz, $2 \times 3'$ -H), 7.43 (br d, 2H, $J = 4.8$ Hz, $2 \times 5'$ -H), 7.91 (d, 2H, $J = 9.0$ Hz, 3 and 5-H). ^{13}C NMR (75.4 MHz, acetone- d_6): δ 53.20 (CH_2), 69.27 (CH_2), 70.65 (CH_2), 70.89 (CH_2), 71.87 (CH_2), 79.17 (CH_2), 112.18 ($\text{C}_2 + \text{C}_6$), 118.37 (C_4), 126.09 ($2 \times \text{C}_{3'}$ and $2 \times \text{C}_{5'}$), 127.57 (C_3 and C_5), 127.96 ($2 \times \text{C}_{4'}$), 147.97 (C_2), 149.23 (C_1). MS (FAB) m/z (%): 526 ($[\text{M} + \text{H}]^+$, 100), 216 (7). HRMS m/z (FAB) for $\text{C}_{27}\text{H}_{31}\text{N}_3\text{O}_4\text{S}_2$ calcd 526.18255; found 526.18288.

Synthesis of Solid Complexes. General Method. The corresponding metal salt ($\text{Cu}(\text{BF}_4)_2$ or $\text{Hg}(\text{CF}_3\text{COO})_2$) (0.2 mmol) was dissolved in abs. ethanol (5 mL) and added to a stirred solution of the respective ligand **2** (0.2 mmol) or **3** (0.1 mmol) in abs. ethanol. The resulting solution was stirred at reflux overnight. The color of the solution changes from colorless to deep red after the addition of the metal ion. The solvent was removed under reduced pressure and the solid was precipitated with the addition of diethyl ether. The solid was separated by centrifugation, washed several times with cold abs. ethanol and diethyl ether and dried under vacuum.

[Cu2](BF₄)₂·2H₂O (4). Color: Red. Yield: 70%. $\text{C}_{37}\text{H}_{51}\text{B}_2\text{CuF}_8\text{N}_3\text{O}_6$, FW = 870.9. Elemental analysis: found C, 47.2; H, 5.3; N, 4.9%. CHNS requires for $\text{C}_{37}\text{H}_{51}\text{B}_2\text{CuF}_8\text{N}_3\text{O}_6$: C, 47.5; H, 5.5; N, 4.5. IR (cm^{-1} ; KBr pellet): ν 3175, 1606, 1513–1495, 1124, 1183. UV-vis in ethanol (λ nm): Band at 336 nm, $\log \epsilon \approx 4.59$. Emission spectra in ethanol ($\lambda_{\text{exc}} = 336$ nm, $\lambda_{\text{em}} = 410$ nm), $\phi_{\text{ethanol}} = 0.65$. MALDI-TOF-MS calcd (found) = $[\text{2Cu}]^+$ 576.7 (576.2), $[(\text{2})_2\text{Cu}]^+$ 1089.0 (1089.5).

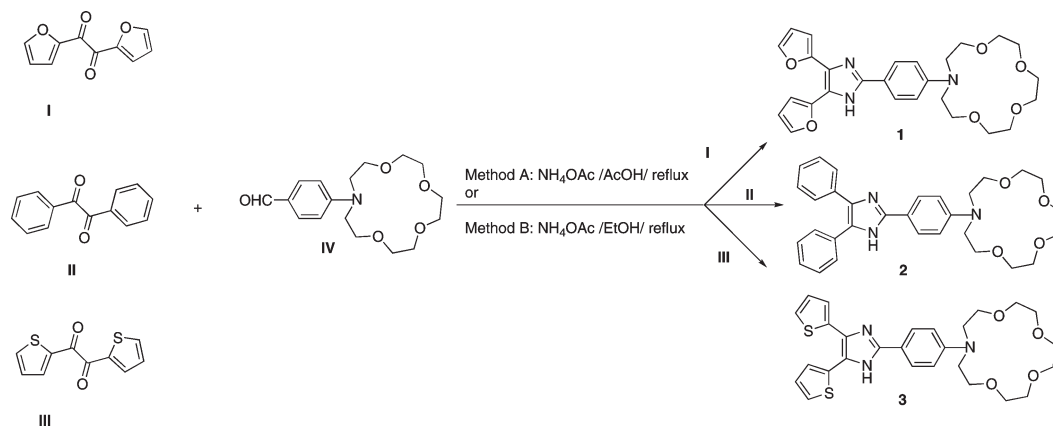
[Cu₂3](BF₄)₄·4H₂O (5). Color: Dark Red. Yield: 79%. $\text{C}_{25}\text{H}_{35}\text{B}_4\text{Cu}_2\text{F}_{16}\text{N}_3\text{O}_8\text{S}_2$, FW = 1044. Elemental analysis: found C, 30.2; H, 4.0; N, 4.0; S, 6.0%. CHNS requires for $\text{C}_{25}\text{H}_{35}\text{B}_4\text{Cu}_2\text{F}_{16}\text{N}_3\text{O}_8\text{S}_2$: C, 30.2; H, 3.7; N, 3.9; S, 5.9. IR (cm^{-1} ; KBr pellet): ν 3087, 1604, 1500–1495, 1107, 1183. UV-vis in ethanol (λ nm): Band at 331 nm, $\log \epsilon \approx 4.43$. Emission spectra in ethanol ($\lambda_{\text{exc}} = 331$ nm, $\lambda_{\text{em}} = 422$ nm), $\phi_{\text{ethanol}} = 0.20$. MALDI-TOF-MS calcd (found) = $[\text{3 Cu}]^+$ 588.6 (588.1), $[(\text{3})_2\text{Cu}]^+$ 1113.8 (1113.4), $[(\text{3})_2\text{Cu}_2]^+$ 1177.4 (1177.3).

[Hg3](CF₃COO)₂ 5H₂O (6). Color: Dark red. Yield: 77%. $\text{C}_{31}\text{H}_{41}\text{F}_6\text{HgN}_3\text{O}_{13}\text{S}_2$, FW = 1043.17. Elemental analysis: found C, 35.4; H, 4.0; N, 4.2; S, 6.5%. CHNS requires for $\text{C}_{31}\text{H}_{41}\text{F}_6\text{HgN}_3\text{O}_{13}\text{S}_2$: C, 35.7; H, 3.9; N, 4.0; S, 6.1. IR (cm^{-1} ; KBr pellet): ν 3097, 1604, 1517–1495, 1107, 1183. UV-vis in DMSO (λ nm): Band at 342 nm, $\log \epsilon \approx 4.74$. Emission spectra in DMSO ($\lambda_{\text{exc}} = 342$ nm, $\lambda_{\text{em}} = 434$ nm), $\phi_{\text{ethanol}} = 0.01$.

Results and Discussion

Synthesis and Characterization of Organic Ligands. The aldehyde precursor **IV**²² was synthesized in 90% yield through Vilsmeier formylation of 13-phenyl-1,4,7,10-tetraoxa-13-aza-cyclopentadecane. Heteroaromatic **I** and **III** and aromatic **II** diones with furyl, thienyl, and aryl groups were used as precursors of imidazo-crown ethers **1–3** to evaluate the effect of the electronic nature of the

(22) Qin, W.; Baruah, M.; Silwa, M.; Van der Auweraer, M.; De Borggraeve, W. M.; Beljonne, D.; Averbek, B. V.; Boens, N. *J. Phys. Chem. A* **2008**, *112*, 6104–6114.

Scheme 1. Synthesis of 2,4,5-Tri(hetero)aryl-imidazo-crown Ether Ligands **1–3**

(hetero)aryl groups on the photophysical and sensory properties of these compounds. Therefore, compounds **1–3** with furyl, aryl, or thienyl moieties linked to the imidazo-crown ether system were synthesized through the condensation of commercially available diones **I–III** with the formyl crown ether derivative **IV** and ammonium acetate (see Scheme 1).^{7i,j,q,23} After the reaction was performed using two different solvents (acetic acid: Method A; or ethanol: Method B) in refluxing conditions (12 h), ethanol gave the highest yields (47–64%) for the synthesis of compounds **1–3** compared to the classical Radziszewski conditions^{7i,j,23} (20–45%). Application of Radziszewski conditions to the synthesis of furyl derivative **1** gave a very complex mixture with decomposition (TLC and ¹H NMR) in which it was not possible to identify the target compound **1**. This compound was only synthesized through method B using mild reaction conditions (Scheme 1).

Complexation reactions between ligands **2** and **3** with the metal salts Cu(BF₄)₂ and Hg(CF₃COO)₂ in refluxing ethanol and in a 1:2 L/M molar ratio for **3** and 1:1 for **2** were carried out to investigate the coordination capability of both ligands in the solid state. Analytically pure products were obtained and formulated as [Cu**2**](BF₄)₂·2H₂O (**4**), [Cu**3**](BF₄)₄·4H₂O (**5**), and [Hg**3**](CF₃COO)₂·5H₂O (**6**). All complexes were obtained in good yield of 70% for **4**, 79% for **5**, and 77% for **6**.

The MALDI-TOF mass spectra of the complexes feature peaks corresponding to the free ligand [LH]⁺, and the fragments [ML]⁺ (L = **2** or **3**), [M₂**3**]⁺, and [M₂**3**]₂⁺. The IR spectra of the complexes were recorded using KBr discs, and all show similar features. After complexation to the metal ion, peaks attributable to the presence of absorption bands from νNH imidazole groups at ~3175 cm⁻¹, and the bands for νC=N groups shift to lower wavenumbers.²⁴ All spectra exhibit medium to strong bands at ~1600 and 1455 cm⁻¹, as expected for the two highest-energy benzene ring vibrations.²⁵ A broad absorption band in the region 3450–3385 cm⁻¹ present in the majority of the complexes is probably due

to the existence of lattice or coordinated water in the complexes.²⁴ A peak due to the BF₄ counterions appears at 1183 cm⁻¹.

Photophysical Studies. The photophysical characterization of compound **1**, **2**, and **3** was performed in acetonitrile, absolute ethanol and dichloromethane. Table 2 summarizes the optical data for all ligands in these protic and aprotic solvents. The absorption and emission band were centered at 328, 320, 325 and 400, 420–440, 440–445 nm, respectively, for **1**, **2**, and **3**. The use of protic and aprotic solvent apparently does not affect the absorption spectra in all cases. However the steady-state luminescence spectra is quenched in aprotic solvents more strongly for compound **1** and **2**, being unaffected for compound **3**. As can be seen in Table 2, compounds **1–3** in the same solvent, absolute ethanol, exhibit quantum yields with values of 0.87 for **1**, 0.35 for **2**, and 0.09 for **3** being the thiophene derivative the less emissive system because of the strong quenching caused by the sulfur atom.²⁶ It is also noteworthy that the substitution of the furyl heterocycle at the 4 and 5 positions of the imidazole system on compound **1** by two aryl rings give rise to a dramatical reduction of the fluorescence probably due to lesser planarity of the aryl-imidazo conjugated system **2**.^{7r}

The same experiment in an aprotic solvent like acetonitrile, showed that all ligands are less emissive, being the fluorescence quantum yields of 0.65 for **1**, 0.07 for **2**, and 0.06 for **3**. The highest value obtained in protic solvents is probably due to protonation of the imidazole nitrogen atom preventing photoinduced electron transfer (PET) phenomena.²⁷

The absorption and emission spectra of compounds **1**, **2**, and **3** in acetonitrile solution are shown in Figure 1. The

Table 2. Optical Data of Compounds **1–3** in Protic and Aprotic Solvents

compounds	solvents	UV–vis			fluorescence	
		λ _{exc} (nm)	Stokes's shift (cm ⁻¹)	log ε	λ _{em} (nm)	φ
1	CH ₃ CN	328	5487	4.69	400	0.65
	EtOH	328	5487	4.69	400	0.87
2	CH ₃ CN	320	8522	4.64	440	0.07
	CH ₂ Cl ₂	320	7440	4.64	420	0.09
3	EtOH	320	7440	4.64	420	0.35
	CH ₃ CN	325	8791	4.55	455	0.06
	CH ₂ Cl ₂	325	8547	4.55	450	0.07
	EtOH	325	8042	4.55	440	0.09

(23) Davidson, D.; Weiss, M.; Jelling, M. J. *J. Org. Chem.* **1937**, 2, 319–327.

(24) Nakamoto, K. *Infrared and Raman Spectra of Inorganic and Coordination Compounds*, 3rd ed.; Wiley-Interscience: New York, 1978.

(25) Peng, S. M.; Gordon, G. C.; Goedken, V. L. *Inorg. Chem.* **1978**, 17, 119–126.

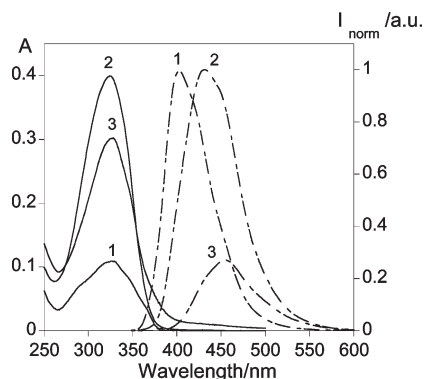


Figure 1. Absorption (full line) and emission spectra (dotted line) of compounds **1–3** in acetonitrile solution. ($[1] = 2.25 \times 10^{-6}$ M, $[2] = 9.05 \times 10^{-6}$ M, $[3] = 8.55 \times 10^{-6}$ M, $\lambda_{\text{exc1}} = 328$ nm, $\lambda_{\text{exc2}} = 320$ nm, $\lambda_{\text{exc3}} = 325$ nm, $T = 298$ K).

insertion of the furan, thiophene, and benzene units in the ligand structure poorly affect the absorption wavelength band. On the other hand, the emission bands showed a noticeable red shift from 400 (**1**) to 455 (**3**) nm, being the highest for the thiophene derivative.

Table 3. Stability Constants with Compounds **1–3** by Hypspec Program^a

	1	2	3
F^-		2.02 ± 0.01 (1:1)	3.06 ± 0.01 (1:1)
Ca^{2+}	4.23 ± 0.01 (1:1)	4.75 ± 0.01 (1:1)	4.16 ± 0.01 (1:1)
Cu^{2+}	11.12 ± 0.01 (1:2)	5.32 ± 0.01 (1:1)	11.58 ± 0.01 (1:2)
Ni^{2+}		4.29 ± 0.02 (1:1)	3.91 ± 0.01 (1:1)
Hg^{2+}	10.04 ± 0.01 (1:2)		6.36 ± 0.01 (1:2)
			8.42 ± 0.3 (1:1)
			11.84 ± 0.3 (1:2)

^a(1:1) = LM. (1:2) = LM₂.

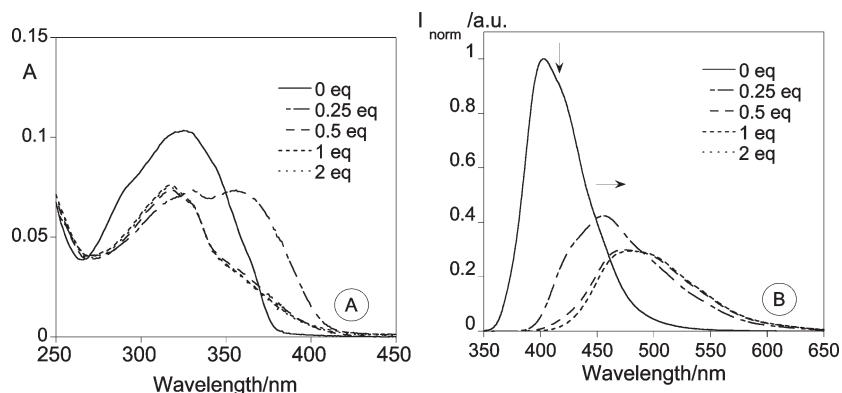


Figure 2. Absorption (A) and emission (B) spectra of compound **1**, with the addition of 0, 0.25, 0.5, 1, and 2 equivalents of methanesulfonic acid. ($T = 298$ K, $[1] = 2.23 \times 10^{-6}$ M, $[\text{CH}_3\text{SO}_3\text{H}] = 1.00 \times 10^{-2}$ M, $\lambda_{\text{exc}} = 328$ nm).

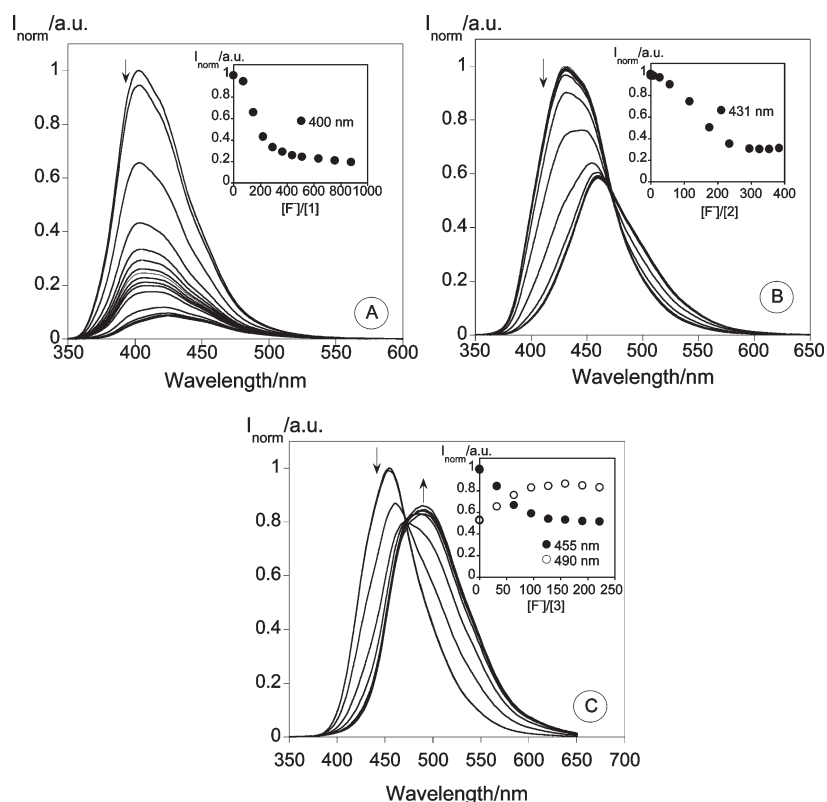


Figure 3. Spectrofluorimetric titrations of compounds **1** (A), **2** (B), and **3** (C), in the presence of F^- , in acetonitrile. The inset represents the emission for **1** (A) at 400 nm, for **2** (B) at 431 nm, and for **3** (C) at 455 and 490 nm.

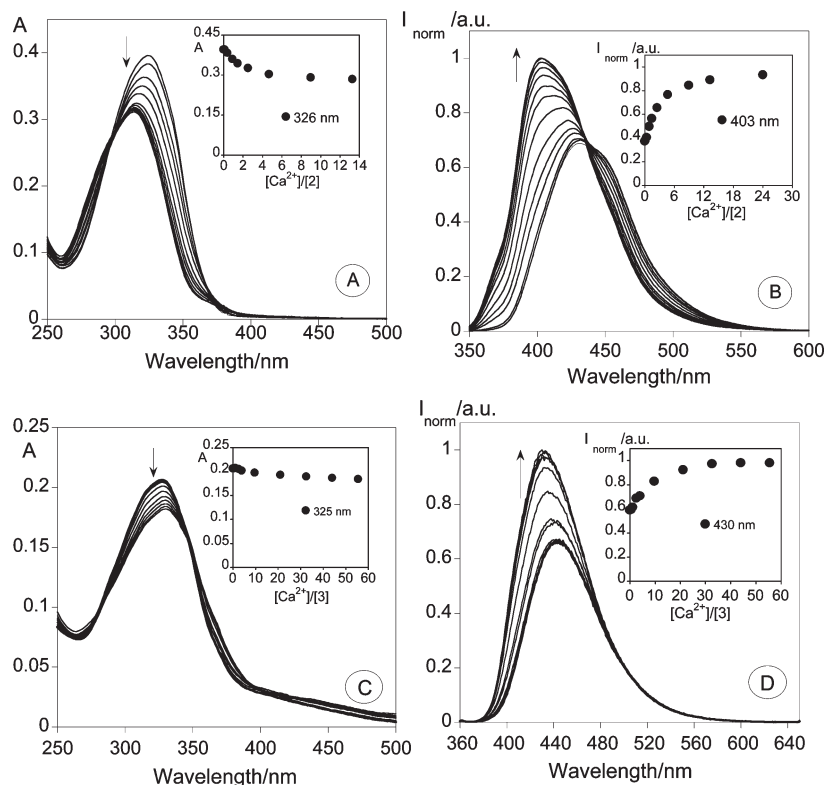


Figure 4. Absorption (A and C) and emission titrations (B and D) of compounds **2** and **3** with the addition of increased amount of Ca^{2+} in acetonitrile (**2**) and absolute ethanol (**3**) solution. The inset represents the absorption at 326 (A) and 325 nm (C) and the emission at 403 (B) and 430 nm (D) as a function of $[\text{Ca}^{2+}]/[\text{2}]$ or $[\text{Ca}^{2+}]/[\text{3}]$. ($[\text{2}] = 9.06 \times 10^{-6} \text{ M}$, $[\text{3}] = 6.34 \times 10^{-6} \text{ M}$, $[\text{Ca}(\text{CF}_3\text{COO})_2] = 1.46 \times 10^{-2} \text{ M}$, $\lambda_{\text{exc2}} = 320 \text{ nm}$, $\lambda_{\text{exc3}} = 325 \text{ nm}$, $T = 298 \text{ K}$).

To explore the sensory ability of systems **1–3** in solution toward H^+ , F^- , Na^+ , Ca^{2+} , Cu^{2+} , Ni^{2+} , and Hg^{2+} , several UV–vis and fluorescence titrations were performed.

The acid–base behavior of compounds **1–3** was studied with the increasing addition of protons using methanesulfonic acid, $\text{CH}_3\text{SO}_3\text{H}$, and fluoride ion as basic anion. The results obtained showed that protonation and deprotonation of the nitrogen present in the azacrown-ether and also at the imidazole nitrogen atom could modulate the fluorescence emission. As an example, in Figure 2 shows the absorption and fluorescence titration of compound **1** with the addition of increasing amount of acid. The fluorescence band was slightly red-shifted and quenched.²⁸ Protonation induced a similar behavior when the parent azacrown **IV** was used, suggesting that the observed quenching in the fluorescence emission is probably because of the formation of a hydrogen-bond interaction between the protonated nitrogen located in the azacrown and the

oxygen atoms, as reported previously for a macrocyclic ligand based on a pseudocrown structure.²⁹

With the addition of the fluoride anion, a small red shift in the absorption spectra for all ligands was observed; at the same time the emission spectra was quenched and red-shifted. Figure 3 shows the fluorescence titrations of **1–3** with the addition of F^- . Taking into account the results observed previously for the protonation of the azacrown nitrogen, deprotonation of this nitrogen should induce a recovery of the fluorescence emission. However, the quenching observed with the addition of a base can be attributed to the deprotonation of the imidazole nitrogen, inducing a PET process from the lone pair of electrons located in this nitrogen atom to the excited chromophore.³⁰ This quenching is similar for imidazo-azacrown derivatives **1–3**. The interaction constants of ligands **2** and **3** with the various ions were calculated and are summarized in Table 3.

15-Crown-5 systems are usually used for the interaction with Na^+ ,³¹ whereas 15-crown-5 monoazacrown ethers

(26) (a) Costa, S. P. G.; Oliveira, E.; Lodeiro, C.; Raposo, M. M. M. *Tetrahedron Lett.* **2008**, 49, 5258–5261. (b) Batista, R. M. F.; Oliveira, E.; Costa, S. P. G.; Lodeiro, C.; Raposo, M. M. M. *Tetrahedron Lett.* **2008**, 49, 6575–6578. (27) Saleh, A.; Al-Soud, Y. A.; Nau, W. M. *Spectrochim. Acta, Part A* **2008**, 71, 818–822.

(28) (a) Lodeiro, C.; Parola, A. J.; Pina, F.; Bazzicalupi, C.; Bencini, A.; Bianchi, A.; Giorgi, C.; Masotti, A.; Valtancoli, B. *Inorg. Chem.* **2001**, 40, 2968–2975. (b) Bazzicalupi, C.; Bencini, A.; Berni, E.; Bianchi, A.; Danesi, A.; Giorgi, C.; Valtancoli, B.; Lodeiro, C.; Lima, J. C.; Pina, F.; Bernardo, M. A. *Inorg. Chem.* **2004**, 43, 5134–5146. (c) Pina, J.; Seixas de Melo, J.; Pina, F.; Lodeiro, C.; Lima, J. C.; Parola, A. J.; Soriano, C.; Clares, M. P.; Albelda, M. T.; Aucejo, R.; Garcia-España, E. *Inorg. Chem.* **2005**, 44, 7449–7458. (d) Pedras, B.; Oliveira, E.; Santos, H.; Rodríguez, L.; Crehuet, R.; Avilés, T.; Capelo, J. L.; Lodeiro, C. *Inorg. Chim. Acta* **2009**, 362, 2627–2635.

(29) (a) NMR titration experiments were carried out in deuterated DMSO, due to the low solubility of **1** in ethanol at NMR concentration, and showed two protonation steps: a first step involving the azacrown nitrogen and a second step involving the imidazole nitrogen. After protonation, both set of signals were broadened and difficult to differentiate. In this case, the signals attributed to the protonated azacrown nitrogen at 3.9–3.4 ppm were stabilized by increasing addition of protons before the signals attributed to the protonated imidazole nitrogen. (b) Vicente, M.; Bastida, R.; Lodeiro, C.; Macias, A.; Parola, A. J.; Valência, L.; Spey, S. E. *Inorg. Chem.* **2003**, 42, 6768–6779.

(30) (a) Yang, T.; Gao, M.; Qin, W.; Yang, J. *Ind. J. Chem. A* **2010**, 49, 45–48. (b) Li, R.-J.; Chang, I.-J. *J. Chin. Chem. Soc.* **2002**, 49, 161–164.

(31) Gokel, G. W.; Leevy, W. M.; Weber, M. E. *Chem. Rev.* **2004**, 104, 2723–2750.

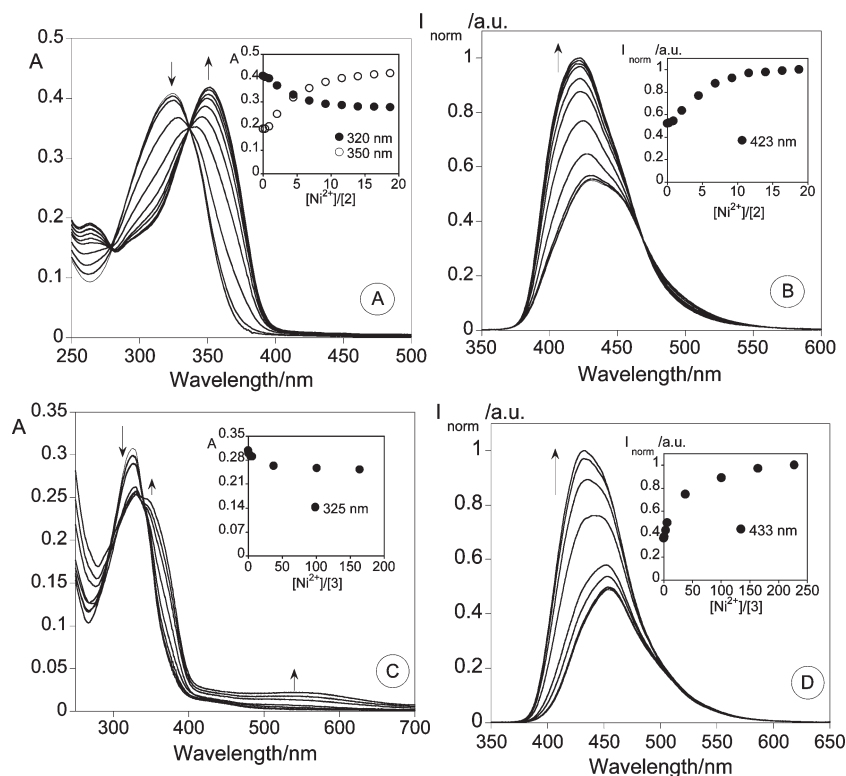


Figure 5. Absorption (A and C) and emission titrations (B and D) of compounds **2** and **3** with the addition of increased amount of Ni^{2+} in acetonitrile. The inset represents the absorption at 320, 350 (A), and 325 nm (C) and the emission at 423 (B) and 433 nm (D) as a function of $[\text{Ni}^{2+}]/[\text{2}]$ or $[\text{Ni}^{2+}]/[\text{3}]$. ($[\text{2}] = 9.06 \times 10^{-6} \text{ M}$, $[\text{3}] = 8.55 \times 10^{-6} \text{ M}$, $[\text{Ni}(\text{BF}_4)_2] = 1.62 \times 10^{-2} \text{ M}$, $\lambda_{\text{exc2}} = 320 \text{ nm}$, $\lambda_{\text{exc3}} = 325 \text{ nm}$, $T = 298 \text{ K}$).

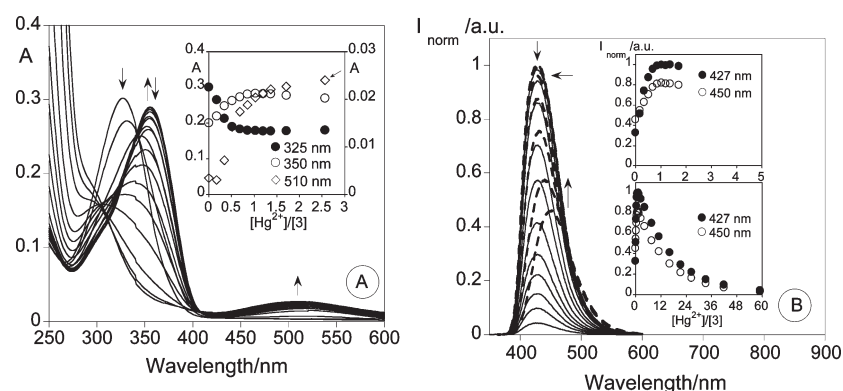


Figure 6. Spectrophotometric (A) and spectrofluorimetric (B) titration of **3** in the presence of Hg^{2+} , in an acetonitrile solution. The inset represents the absorption (A) at 325, 350, and 510 nm and the emission (B) at 427 and 450 nm, as a function of $[\text{Hg}^{2+}]/[\text{3}]$. ($[\text{3}] = 6.66 \times 10^{-6} \text{ M}$, $[\text{Hg}(\text{CF}_3\text{COO})_2] = 1.7 \times 10^{-2} \text{ M}$, $\lambda_{\text{exc3}} = 325 \text{ nm}$, $T = 298 \text{ K}$).

show better results for Ca^{2+} .³² In this case, compounds **1–3** did not show any changes in the ground state (absorption) and in the excited state (emission) after addition of Na^+ . However, in the presence of Ca^{2+} ligands **2** and **3** in acetonitrile or absolute ethanol, respectively, showed a blue shift in the absorption spectra and an enhancement of the fluorescence emission (see Figure 4). The complexation constants with Ca^{2+} were calculated using the program HYPSPPEC³³ and are summarized in Table 3. In all cases, the constants suggest the formation of a mononuclear complex with a value between $\log \beta 4.75 \pm 0.01$ for **2** and $\log \beta 4.16 \pm 0.01$ for **3**.

Following our exploration of the different coordination sites present in ligands **1–3**, the second site to be explored will be the nitrogen atom located at the imidazole ring. This imidazole nitrogen atom can form a chelate unit with the potential coordinative oxygen or sulfur atoms present in the furan **1** or thiophene **3** heterocycles. To explore the interaction of transition (Cu^{2+} and Ni^{2+}) and post-transition (Hg^{2+}) metal ions with this coordination site, several metal titrations were performed.

With the addition of Ni^{2+} , only ligands **2** and **3** showed a red shift on the absorption spectra and an enhancement on the fluorescence emission intensity (Figure 5). The complexation constants fit to a mononuclear species for ligand **2** with a value of $\log \beta 4.29 \pm 0.02$, and to

(32) Warmke, H.; Wicz, W.; Ossowski, T. *Talanta* **2000**, *52*, 449–456.

(33) Gans, P.; Sabatini, A.; Vacca, A. *Talanta* **1996**, *43*, 1739–1753.

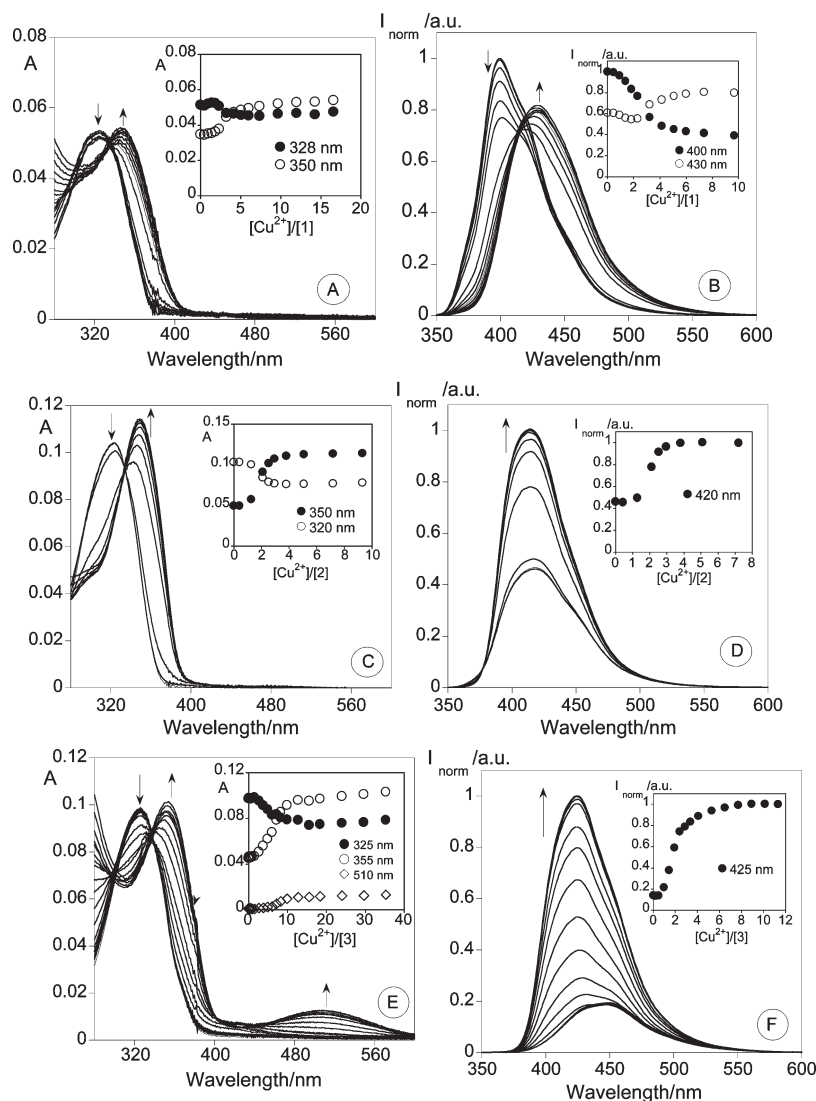


Figure 7. Absorption (A, C, and E) and emission titrations (B, D, and F) of compounds 1–3 with the addition of increased amount of Cu^{2+} in absolute ethanol. The inset represents the absorption at 328 and 350 nm for A, 320 and 350 nm for C, and 325, 355, and 510 nm for (E), and the emission at 400, 430 (B), 420 (D), and 425 nm for (F) as a function of $[\text{Cu}^{2+}]/[\text{1}]$, $[\text{Cu}^{2+}]/[\text{2}]$, $[\text{Cu}^{2+}]/[\text{3}]$ respectively. $[\text{1}] = 1.49 \times 10^{-6}$ M, $[\text{2}] = 1.62 \times 10^{-6}$ M, $[\text{3}] = 2.05 \times 10^{-6}$ M, $[\text{Cu}(\text{BF}_4)_2] = 1.62 \times 10^{-2}$ M, $\lambda_{\text{exc1}} = 328$ nm, $\lambda_{\text{exc2}} = 320$ nm, $\lambda_{\text{exc3}} = 325$ nm, $T = 298$ K).

mononuclear and dinuclear species for compound 3 with values of $\log \beta$ 3.91 ± 0.01 and 6.36 ± 0.01 , respectively. It is important to note that for compound 3 after formation of the dinuclear species, a colored band centered at ~ 550 nm was developed. This band could be attributable to a tetracoordinated Ni^{2+} complexes.³⁴

Taking into account the presence of two thiophene rings in ligand 3, addition of a soft-metal ion³⁵ could be used to explore the involvement of the sulphur atoms in the complex stabilization. Figure 6 represents the absorption and emission titrations of compound 3 with addition of Hg^{2+} . The absorption spectra showed a remarkable red shift and the formation of band centered at ~ 510 nm, with the color of the final solution turning pale pink. At the same time the fluorescence increased with the addition of one metal ion equivalent, followed by an intense decrease with further metal addition. This final quenching could be

attributed to a partial reabsorption of the emitted light by the colored complex and by the heavy atom effect via the enhancement of spin–orbit coupling.³⁶ The complexation constants are summarized in Table 3.

The most interesting results arise from the interaction with Cu^{2+} . All ligands were explored in the presence of Cu^{2+} in an absolute ethanol solution to prevent the self-reduction to Cu^+ sometimes observed in acetonitrile.³⁷ For all cases, an enhancement of the fluorescence emission at 430 nm was observed (see Figure 7). The absorption spectrum showed a red shift with the formation of well-defined isosbestic points at 333, 334, and 336 nm, for

(36) (a) McClure, D. S. *J. Chem. Phys.* **1952**, *20*, 682–686. (b) Burress, C. N.; Bodine, M. I.; Elbeirami, O.; Reibenspies, J. H.; Omary, M. A.; Gabbai, F. P. *Inorg. Chem.* **2007**, *46*, 1388–1395. (c) Marnett, M.; Lippolis, V.; Caltagirone, C.; Capelo, J. L.; Nieto-Faza, O.; Lodeiro, C. *Inorg. Chem.* **2010**, *49*(18), 8276–8286. doi:10.1021/ic1007439. (d) Tamayo, A.; Pedras, B.; Lodeiro, C.; Escriche, L.; Casabó, L.; Capelo, J. L.; Covelo, B.; Kivekäs, R.; Sillanpää, R. *Inorg. Chem.* **2007**, *46*, 7818–7826.

(37) (a) Beloglazkina, E. Z.; Shimorsky, A. V.; Mazhuga, A. G.; Shilova, O. V.; Tafenko, V. A.; Zyk, N. V. *Rus. J. Gen. Chem.* **2009**, *79*, 1504–1508. (b) Milne, J. B. *Can. J. Chem.* **1970**, *48*, 75–79.

(34) Lever, A. B. P. *Inorganic Electronic Spectroscopy*; Elsevier: Amsterdam, 1968.

(35) Pearson, R. G. *J. Am. Chem. Soc.* **1963**, *22*, 3533–3539.

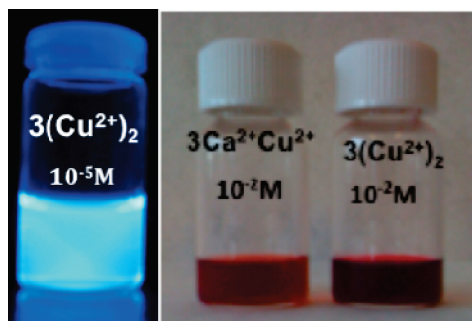


Figure 8. (Right) Ethanol solutions of compound **3** in the presence of one equivalent of Cu^{2+} and Ca^{2+} , and in the presence of two equivalents of Cu^{2+} . (Left) Emission under irradiation at 365 nm of an ethanolic solution of compound **3** in the presence of 2 equiv of Cu^{2+} .

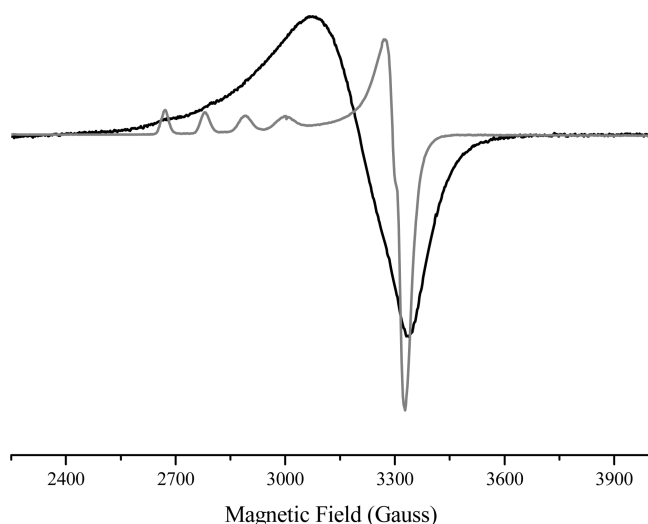


Figure 9. EPR spectra of compound $[\text{Cu}_23](\text{BF}_4)_4 \cdot 4\text{H}_2\text{O}$ (**5**) recorded in a polycrystalline powdered sample (black) and dissolved in acetonitrile (gray). Simulation of the solution spectrum yields the EPR parameters: $g_1 = 2.435$, $g_2 = 2.097$, $g_3 = 2.074$, $A_1 = 110$ G. Simulation was performed using Simfonia v1.25 (Bruker, Inc.).

1–3 respectively. This result indicates that the stoichiometry of the reaction remains unchanged during the chemical reaction and no secondary reactions occur during the considered time range.

For compound **3** a visible band centered at 510 nm was observed. Nevertheless, as previously discussed for the Hg^{2+} complex, this fact did not influence the fluorescence emission, and the final complex formed was highly emissive with a fluorescence quantum yield of 0.48. The complexation constants for all cases are summarized in Table 3. The highest values were obtained for compounds **1** and **3**, and agree with the formation of dinuclear species. However due to the instability observed in the complex with compound **1** bearing furyl substituent, further studies with this complex were prevented.

As is well-known, copper complexes with brown-red color can be understood as complexes with Cu^+ .³⁸ Because of the deep dark red color observed in the complex with ligand **3** (see Figure 8), additional studies concerning the oxidation state of the metal centers was performed by

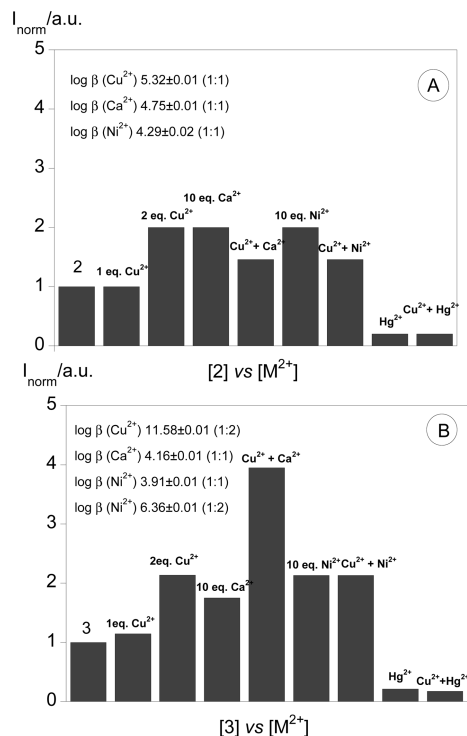


Figure 10. Normalized fluorescence of compounds **2** (A) and **3** (B) in the presence of Cu^{2+} , Ca^{2+} , Ni^{2+} , and Hg^{2+} , in absolute ethanol.

NMR and EPR spectroscopy. The NMR spectra in acetonitrile- d_3 revealed a group of very broad signals, suggesting the presence of Cu^{2+} paramagnetic centers.

The EPR solution spectra (see Figure 9) showed the same behavior for all Cu^{2+} paramagnetic complexes. Simulation of the solution spectrum yielded the EPR parameters: $g_1 = 2.435$, $g_2 = 2.097$, $g_3 = 2.074$, $A_1 = 110$ G in all cases. These results suggest that the two metal centers present in the complex with ligand **3** are in similar environment coordination sites. It can be postulated that one metal could be located in the azacrown unit, coordinated to the nitrogen atom and at least four oxygen atoms, and the second metal center could be located in the imidazole ring, coordinated to the imidazole nitrogen completing the coordination sphere with several water molecules. The presence of these water molecules was proved also by the infrared spectra in KBr pellets.

As ligand **3** can be coordinated by two metal ions, the formation of heterodinuclear species by the addition of Ca^{2+} followed by one Cu^{2+} equivalent was explored. The color of the complex changes from deep dark red to orange.

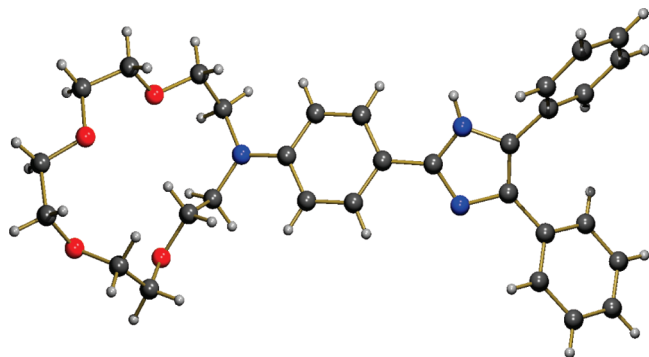
The fluorescence quantum yield for the dinuclear Cu^{2+} complex synthesized with **3** was 0.48; for comparison purposes, the addition of 1 equiv of Cu^{2+} , followed by the addition of Ca^{2+} lead to a more emissive species with fluorescence quantum yield of 0.79. Taking into account that Ca^{2+} will be coordinated to the azacrown, the Cu^{2+} center must be now located at the imidazole ring.

To explore the effect of simultaneous coordination on the fluorescence emission of ligands **2** and **3**, several competitive experiments were performed in absolute ethanol. As was discussed previously, in ethanol the imidazole nitrogen is partially or totally protonated preventing the PET effect. Careful inspection of Figure 10A shows that addition of Cu^{2+} , Ni^{2+} , and Ca^{2+} to ligand **2**

(38) (a) Strange, A. F.; Klein, A.; Klinkhammer, K.-W.; Kaim, W. *Inorg. Chim. Acta* **2001**, *324*, 336–341. (b) Rapenne, G.; Dietrich-Buchecker, C.; Sauvage, J.-P. *J. Am. Chem. Soc.* **1999**, *121*, 994–1001.

Table 4. Luminescence Quantum Yield of Compound **3** in the Presence of Ca^{2+} and Cu^{2+}

species	quantum yield, ϕ
3	0.07
3 + Cu^{2+}	0.48
3 + Ca^{2+}	0.30
3 + Cu^{2+} + Ca^{2+}	0.79

**Figure 11.** X-ray crystallographic structures of compound **2**.

induced an one-fold increase of the fluorescence intensity (observed previously in the metal titrations) and after addition of pairs $\text{Cu}^{2+}/\text{Ca}^{2+}$ and $\text{Cu}^{2+}/\text{Ni}^{2+}$ a small decrease of the intensity was observed. Finally, as expected, addition of Hg^{2+} and the pair $\text{Cu}^{2+}/\text{Hg}^{2+}$ quenched the fluorescence emission.

In Figure 10B are shown the results of the same experiments for ligand **3**. An enhancement of the fluorescence emission was observed after coordination by two equivalent of Cu^{2+} with similar intensity as observed for the pair $\text{Cu}^{2+}/\text{Ni}^{2+}$. This CHEF effect was also observed for the addition of Ca^{2+} , being more intense when the pair $\text{Cu}^{2+}/\text{Ca}^{2+}$ was used.

To use compound **3** as fluorescent chemosensor for Cu^{2+} in solution, the detection (DL) and quantification (QL) limits were determined in absolute ethanol.

The values obtained at 510 nm, where the visible band was formed, was of 0.003 ± 0.001 (DL) and 0.007 ± 0.002 (QL). Taking into account these results, the minimal amount of Cu^{2+} that could be determined in absolute ethanol is 1.60 ppm.

Crystallography Data. Crystals of compound **2** (Figure 11) suitable for X-ray diffraction were obtained by slow evaporation of an ethanolic solution. Bond distances and angles are all within the normal ranges. The modified azacrown ethers

adopt a nearly planar conformation, with the four oxygen and the nitrogen atoms of the molecule describing a slightly distorted plane. The dihedral angle between the planes containing the phenyl and the imidazolyl units are 121° , while between the planes containing the phenyl and the crown-ether units are 122° .

Conclusions

A new family of emissive molecular probes **1–3**, derived from 15-crown-5 monoaza macrocyclic ligands bearing a furyl, aryl or thienyl 4,5-disubstituted imidazole system have been synthesized in good to excellent yields by a simple reaction, and their photophysical properties have been evaluated in solution and in solid state by absorption and fluorescence emission spectroscopy and by MALDI-TOF-MS spectrometry in the gas phase.

Their capacity to act as potential sensors for divalent metal ions Ca^{2+} , Cu^{2+} , Ni^{2+} and Hg^{2+} was explored in solution and in solid state. Interesting results were found for compound **3** bearing the thiophene rings being an example of enhancement of fluorescent emission upon coordination to Cu^{2+} , Ni^{2+} or Ca^{2+} . The complex $(\text{CuCa3})^{4+}$ in solution was the most emissive with a fluorescence quantum yield of 0.79.

Acknowledgment. We are indebted to *InOU Uvigo* by project K914 122P 64702 (Spain) and FCT-Portugal by project PTDC/QUI/66250/2006 for financial support. The NMR spectrometers are part of the National NMR Network and were purchased in the framework of the National Programme for Scientific Re-equipment, contract REDE/1517/RMN/2005, with funds from POCI 2010 (FEDER) and FCT-Portugal. C.L. thanks Xunta de Galicia, Spain, for the Isidro Parga Pondal Research Program. E.O. and R.B. thank FC-MCTES (Portugal) by their PhD grants SFRH/BD/35905/2007 and SFRH/BD/36396/2007, respectively. We are grateful to Dr. Cristina Nuñez and Dr. Pablo González from the REQUIMTE, Universidade NOVA de Lisboa, Portugal, for their important help with the crystallographic and EPR data, respectively, and Dr. José Luis Capelo from the University of Vigo, Spain, for the help with the MALDI-TOF-MS spectra.

Supporting Information Available: X-ray crystallographic data of **2** in CIF format and Job's plot for compound **3** in the presence of Cu^{2+} . This material is available free of charge via the Internet at <http://pubs.acs.org>.